THE INFLUENCE OF THE GROUND SPATIAL VARIABILITY ON THE SETTLEMENTS CAUSED BY TUNNEL EXCAVATION

L'INFLUENCE DE LA VARIABILITE SPATIALE DES PROPRIETES GEO-TECHNIQUES SUR L'AMPLITUDE DES DÉPLACEMENTS EN RAISON DE LE CROISEMENT DES TUNNELS

Miranda, Luís, LNEC, Portugal, lmiranda@lnec.pt
Bilé Serra, João, LNEC, Portugal, biles@lnec.pt

1. INTRODUCTION

Ground settlements caused by the excavation of tunnels may be particularly relevant in urban areas, with greater relevance in soft soils. Estimating the amplitude of the settlements and the associated risk of damage to buildings is an essential part of tunnel planning, design and construction. Empirical, analytical and numerical models, with judiciously chosen parameters, are currently used. However, the local (statistical) variability and the spatial variability are not generally considered. The quality of the settlement estimates depends on the amplitude of both types of variability, among other factors. The quantification of ground variability and its consideration on the surface settlements estimation improves its robustness. This is an important issue regarding the forecasts for the definition of warning and alarm limits for risk management during tunnel construction.

2. SURFACE SETTLEMENTS DUE TO TUNNEL EXCAVATION

2.1 Geometry of subsidence

As outlined by Mair and Taylor (1997) ground movements due to TBM tunneling may have different origins, namely: (i) extrusion of the ground at the face, (ii) radial motion towards the shield, due to over excavation of soil, (iii) convergence at the tail of the TBM (usually the most influential), (iv) convergence due to the deformation of the liner, and (v) radial deformation in soft soils due to time lagged effects. As far as NATM tunneling is concerned, movements can be assigned to: i) ground extrusion at the face, (ii) radial convergence of the lining and, (iii) of the ground due to ground consolidation.

The geometry of the subsidence basin and the amplitude of surface settlements caused by underground excavation can be estimated with a reasonable degree of confidence for the green field situation. Empirical correlations based on field observations are currently used for this estimation.

In practice, however, movement patterns may be affected by structures. If their influence is significant, one will have to resort to numerical methods which take into account three-dimensional effects and structural models, even if these are simple models.
In Figure 1 the geometry of the subsidence basin is outlined, with a reference system xyz in which x and z are the orthogonal axes in the transverse plane of the face and y is the longitudinal axis, The vertical displacement is designated by S_v and the horizontal displacements in the transverse and longitudinal directions, by S_{hx} and S_{hy}.

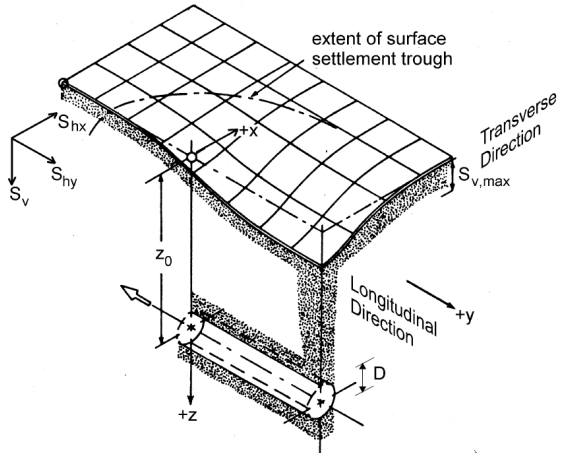

Figure 1 – Geometry of the subsidence basin (adapted from Franzius, 2003)

According to Schmidt (1969) and Peck (1969), the cross-sectional area of subsidence at the surface can be described by a Gaussian error function:

$$S_v(x) = S_{v,max} e^{-\frac{x^2}{2i_x^2}} \quad [1]$$

where $S_{v,max}$ is the peak settlement over the tunnel axis. The parameter i_x stands for the distance between the plane of symmetry of the tunnel and the inflexion points of the theoretical subsidence curve (see Figure 2).

The volume of surface subsidence per unit length of the tunnel is obtained by integrating equation [1]:

$$V_S = \int_{-\infty}^{+\infty} S_V(x)dx = \sqrt{2\pi} i_x S_{V,máx} \quad [2]$$

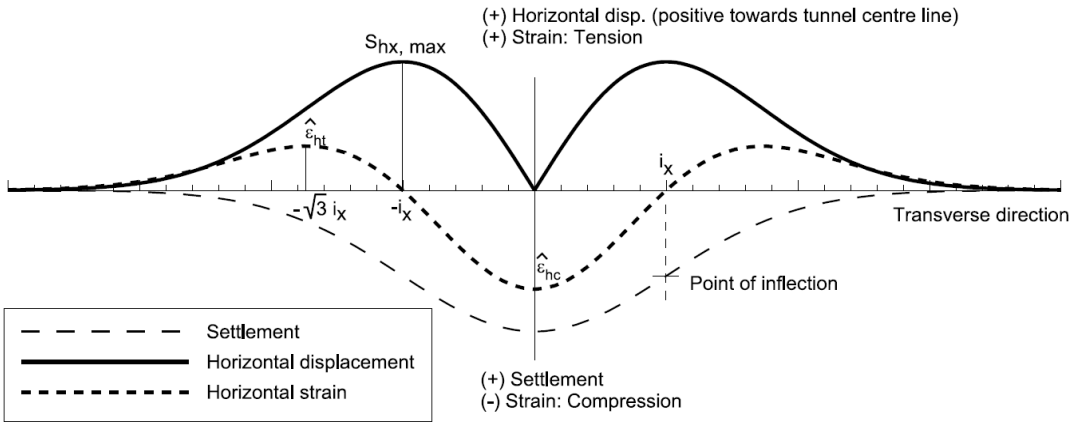

Figure 2 – Transverse subsidence curve: settlements, horizontal displacements and horizontal extension (Franzius, 2003).

The difference between this volume and the so called lost volume towards the tunnel perimeter V_L reflects the occurrence of dilatancy in the ground. They may be assumed as equal in undrained conditions. Combining the unit volume of subsidence v_S (ratio of V_S to the theoretical cross-sectional area of the tunnel) with i_x, it is possible to express the settlement in a generic position x as

$$S_V(x) = \frac{A_t v_S}{\sqrt{2\pi} i_x} e^{-\frac{x^2}{2i_x^2}} \qquad [3]$$

2.2 Modelling with analytical expressions

The use of elastoplastic models for modelling the subsidence pattern, either analytical or numerical, is strictly required by the non-linearity and partial irreversibility of deformation that characterizes the mechanical response of the ground. At sufficiently distant positions from the excavation, however, the use of elastic models based on an estimate of the ground loss may be appropriate. Several models may be found in the literature such as the one by Sagaseta (1987), for ground loss estimate due to tunnel construction (valid for a constant volume condition), which was later extended by Verruijt and Booker (1996) to allow the use of an arbitrary value of the Poisson's ratio. In this extended solution the joint effects of radial contraction and ovalization of the tunnel are considered.

Loganathan and Poulos (1998) further developed the solution by Verruijt and Booker and defined an equivalent parameter ε_{eq}, related to the pure contraction of the tunnel, based on the gap parameter introduced by Rowe and Knack (1983). According to Lee et al. (1992), this parameter results from the combined effects of three-dimensional elastoplastic deformations at the tunnel face (U_{3D}), from the soil over-excavation (ω) and also from the gap due to the conical shape of the tunneling machine (G_p):

$$g = G_p + U_{3D} + \omega \qquad [4]$$

The gap G_p is the sum of twice the thickness of the TBM tail (Δ) with the initial gap between the ground and the tail (ζ), i.e. $G_p = 2\Delta + \zeta$. The gap can be reduced to a negligible dimension if contact grouting is used. However, given the shrinkage of the grout, it is generally assumed that a residual value of 7 to 10% of the initial gap still remains. Shrinkage is considered to develop in undrained conditions, since it occurs in a short period of time. The parameter U_{3D} is defined as

$$U_{3D} = \frac{k}{2}\delta_X \qquad [5]$$

where k is a soil-cutter resistance factor, ranging from 0.7 to 0.9 for stiff to soft clays and being equal to 1 for very soft clays (Lee et al., 1992). δ_X stands for half of the convergence at the tunnel face

$$\delta_X = \frac{\Omega R \sigma_0}{E} \qquad [6]$$

where Ω is a dimensionless displacement related factor, R is the tunnel radius, E is the deformability modulus of the soil (typically, the undrained modulus in extension E_u) and $\sigma_0 = K_0\sigma'_V + \sigma_W - \sigma_i$. In this expression K_0 is effective coefficient of earth pressure at rest, σ'_V is the vertical effective stress due to the overburden, σ_W is the pore-water pressure at the spring line of the tunnel and σ_i is the tunnel support pressure at the face.

Finally, the parameter ω is related to the over-excavation caused by the bead. It is equal to ω^* if there is no bead or to the sum of ω^* with the thickness or twice the thickness of the bead, whether the bead spans 180º of the hood or covers the full circumference, respectively.

The smallest of $0.6G_p$ and $U_i/3$ is chosen and deignated as ω^*, where U_i is the radial plane strain displacement of the ground, defined as:

$$\frac{U_i}{R} = 1 - \left[1 + \frac{2(1+\nu_u)S_u}{E_u} e^{N-1}\right]^{-1/2} \qquad [7]$$

in which E_u e ν_u are respectively the undrained deformability modulus and Poisson's ratio, s_u is the undrained strength and N is the stability number.

The parameter ε_{eq} incorporates in its definition the nonlinear ground movement due to the tunnel ovalization. It is defined as

$$\varepsilon_{eq} = \frac{4gR + g^2}{4R^2} \exp\left[-\frac{1.38x^2}{(z_0 + R)^2} - \frac{0.69z^2}{z_0^2} \right] \quad [8]$$

The undrained surface settlement is equal to

$$S_V = 4(1-\nu)R^2 \frac{z_0}{x^2 + z_0^2} \frac{4gR + g^2}{4R^2} \exp\left[-\frac{1.38x^2}{(z_0 + R)^2} \right] \quad [9]$$

3. ASSESSMENT OF THE GROUND GEOTECHNICAL PROPERTIES VARIABILITY

The variability of the soil is caused by the natural geological processes that modify the ground. It can be observed locally – statistical variability – or considering the values in several positions – spatial variability.

3.1 Statistical characterization of the geotechnical parameters

3.1.1 Statistical measures of position, local dispersion and spatial correlation

The spatial variability of the ground can be modelled taking into account two contributions: a known deterministic trend and a residual variability about that trend, which characterizes the inherent variability of the soil deposit. For the one-dimensional model case, the local value of the property $z(x)$ can be represented by:

$$z(x) = t(x) + u(x) \quad [10]$$

in which $t(x)$ is the value of the statistical trend at x and $u(x)$ is the residual variation, suppletive to the tendency. The residuals u are characterized statistically as a random variable, with zero mean, and variance:

$$\mathrm{Var}(u) = E\left[\{z(x) - t(x)\}^2\right] \quad [11]$$

The variance of the residuals reflects the uncertainty about the difference between the interpolation trend and the actual value of soil properties.

The remaining spatial structure, after removing the trend, shows the existence of correlation among the residuals, ie, the residuals aren't statiscally independent. The positive residuals tend to group, as well as the negative ones. This spatial structure of variation, unconsidered by the trend, may be described by the spatial correlation, usually called autocorrelation, which decreases with the distance between positions. The strenght and the signal of the correlation between two scalar variables z_1 and z_2 are measured by the correlation coefficient $\rho(z_1, z_2)$. The two variables might represent different but related properties or the same property in distinct locations. In the latter case, in which the covariance and the correlation depend on the separation distance, they are designated by autocovariance and autocorrelation, respectively.

The correlation coefficient ρ is equal to one for zero separation distance and tends assimptotically to zero for increasing separation distances. Therefore, the spatial variability about a trend is due to the variance (local effect) and to the autocorrelation (spatial effect).

The spatial association of residuals may be summarized by the autocorrelation function $R_z(\delta)$, which describes the correlation of $u(x_i)$ and $u(x_j)$ as separation distance δ increases:

$$R_z(\delta) = \frac{1}{\mathrm{Var}[u(x)]} E[u(x_i)u(x_i + \delta)] = \frac{C_z(\delta)}{\mathrm{Var}[u(x)]} \quad [12]$$

in which $\mathrm{Var}[u(x)]$ is the variance of the residuals and $C_z(\delta)$ is the autocovariance function of the residuals spaced at distance δ. In practice, simplificative hypotheses are assumed about the autocorrelation, namely in what concerns isotropy and stationarity, which is equivalent to considering the deposit statistically homogeneous.

For the purposes of modeling and analysis, it is usually convenient to choose infinitely differentiable functions to represent $R_z(\delta)$. Functions commonly used to represent autocorrelation are shown in Table 1, in which δ_0 is a constant having units of length. These functions are graphically presented in Figure 3.

Table 1 – One-dimensional models of autocorrelation (adapted from Baecher and Christian, 2003)

Model	Equation
White noise (R1)	$R_z(\delta) = \begin{cases} 1, \delta = 0 \\ 0, \text{otherwise} \end{cases}$
Linear (R2)	$R_z(\delta) = \begin{cases} 1 - \lvert\delta\rvert / \delta_0, \delta \le \delta_0 \\ 0, \text{otherwise} \end{cases}$
Exponential (R3)	$R_z(\delta) = \exp\left(-\lvert\delta\rvert / \delta_0\right)$
Squared exponential (R4)	$R_z(\delta) = \exp\left(-\left(\lvert\delta\rvert / \delta_0\right)^2\right)$

In order to integrate spatial variability in models of superficial settlements caused by tunnel excavation, it is necessary to resort to the random field theory, considering that the generic variable $z(x)$ (e.g., the deformability modulus) is a realization of a random field. A random field is defined by the joint probability distribution, which describes the variation of z within the space S_x:

$$F_{x_1,\ldots,x_n}(z_1,\ldots,z_n) = P\{z(x_1) \le z_1,\ldots,z(x_n) \le z_n\} \quad [13]$$

Should the random field be assumed second-order stationary and isotropic the autocovariance function depends only on the distance $\delta = \lvert x_i - x_j \rvert$ between the points. The functions $R_z(\delta)$ and $C_z(\delta)$ become even and limited, i.e., respectively

$$C_z(\delta) = C_z(-\delta); R_z(\delta) = R_z(-\delta) \text{ and} \quad [14]$$

$C_z(\delta) \le C_z(0) = \sigma^2; |R_z(\delta)| \le 1$

A random field that doesn't meet the stationarity conditions is said to be non-stationary, i.e., it is statistically heterogeneous. Stationarity usually depends upon scale. Within a small region, such as a building foundation, soil properties may behave as if drawn from a stationary process; whereas, that may not happen over a larger region. Another property that is used to characterize a random field is ergodicity. Basically, ergodicity means that the probabilistic properties of a random process (field) can be completely estimated from observing one realization of that process; it implies strict stationarity.

Let us then consider the stochastic scalar field $z(x)$, with the usual properties assumed in the random field theory: homogeneity, isotropy, ergodicity and stationarity. Its parameters are, thus, the mean μ_z, assumed constant, the variance σ_z^2 and the auto-covariance function $C_z(\delta)$ (Baecher and Christian, 2003).

The average process in a reference length X is an essential resource in geotechnical modelling, allowing to define "homogeneous" sub-domains. As a matter of fact, the vast majority of the considered information on geotechnical parameters in any site is defined over a finite domain and represents a local average of the parameter, instead of its exact local value. The spatial average of the process within the interval $[0, X]$ is:

$$M_X(z(x)) = \frac{1}{X}\int_0^X z(x)\, dx \qquad [15]$$

The spatial averaging process smoothes the studied variables. In fact, the variance of the averaged process is smaller and its spatial correlation is wider than the original process $z(x)$. The corresponding moments of the spatial mean of order 1 and 2 can be determined from the mean and variance of the scalar process $z(x)$:

$$E[M_X] = \mu_{M_X} = \frac{1}{X}\int_0^X \mu_z\, dx = \mu_z \qquad [16]$$

$$Var[M_X] = \frac{2}{X^2}\int_0^X (X-\delta) C_z(\delta)\, d\delta \qquad [17]$$

The autocovariance of the average process is given by:

$$C_{M_X}(\delta) = \frac{1}{X^2}\int_0^X \int_0^X C_z(\delta + x_i - x_j)\, dx_i dx_j \qquad [18]$$

The reduction in variance due to the averaging may be represented by a variance reduction function $\Gamma_z^2(X)$ that depends on the autocorrelation function $R_z(\delta)$ and the width of the observation window X:

$$\Gamma_z^2(X) = \frac{Var[M_X(z(x))]}{Var[z(x)]} = \frac{2}{X}\int_0^X \left(1 - \frac{\delta}{X}\right) R_z(\delta)\, d\delta \qquad [19]$$

The scale of fluctuation or (effective) correlation distance θ_z of the process $z(x)$ represents the distance above which the function $R_z(\delta)$ takes values lower than $1/e^2$, i.e. where no significant correlation exists. According to Vanmarcke (1984) the scale of fluctuation can be estimated by:

$$\theta_z = \lim_{X\to\infty} X\, \Gamma_z^2(X) \qquad [20]$$

That is, θ_z / X is the infinite asymptote of $\Gamma_z^2(X)$, meaning that $R_z(\delta) \to 0$ when $\delta \to \infty$. In this case, θ_z can be found through:

$$\theta_z = 2\int_0^\infty R_z(\delta) d\delta = \int_{-\infty}^\infty R_z(\delta) d\delta \qquad [21]$$

For the models which autocorrelation function was described in Table 1, the variance reduction functions and the corresponding scales of fluctuation are presented in Table 2. These functions are graphically presented in Figure 3.

Table 2 – Variance reduction functions for one-dimensional models of autocorrelation (adapted from Baecher and Christian, 2003)

Model	Variance reduction function	θ_z
White noise ($\Gamma 1$)	$\Gamma_z^2(X) = \begin{cases} 1, X = 0 \\ 0, \text{otherwise} \end{cases}$	0
Linear ($\Gamma 2$)	$\Gamma_z^2(X) = \begin{cases} 1 - X/3\delta_0, X \le \delta_0 \\ (\delta_0/X)(1 - \delta_0/3X), o. \end{cases}$	δ_0
Exponential ($\Gamma 3$)	$\Gamma_z^2(X) = 2\left(\frac{\delta_0}{X}\right)^2\left(\frac{X}{\delta_0} - 1 + \exp\left(-\frac{X}{\delta_0}\right)\right)$	$2\delta_0$
Square exponential ($\Gamma 4$)	$\Gamma_z^2(X) = \left(\frac{\delta_0}{X}\right)^2\left(\sqrt{\pi}\frac{X}{\delta_0} erf\left(\frac{X}{\delta_0}\right) - 1 + \exp\left(-\left(\frac{X}{\delta_0}\right)^2\right)\right)$ in which *erf* is the error function	$\sqrt{\pi}\delta_0$

3.1.2 Literature values of statistical measures

The observations of the ground parameters suggest a considerable variability, not only from zone to zone, but also inside each presumed homogeneous deposit. The variability of the ground, modelled using the random field theory, can be described with the coefficient of variation (COV_z) and the fluctuation scale θ_z.

The spatial variability pattern is related with the specific regional geology of a certain zone. Thus, the ground variability data set shall always be locally gathered. Still, published values of variation interval of COV for geotechnical variables may be useful as an introductory guidance (see Table 3). Caution must be taken, however, for these values are likely overestimated for the following reasons: (i) the joint consideration of contrasting geological

units in the same sample; (ii) measuring errors, (iii) diversity of equipments and interpretation methods and (iv) presence of deterministic trends.

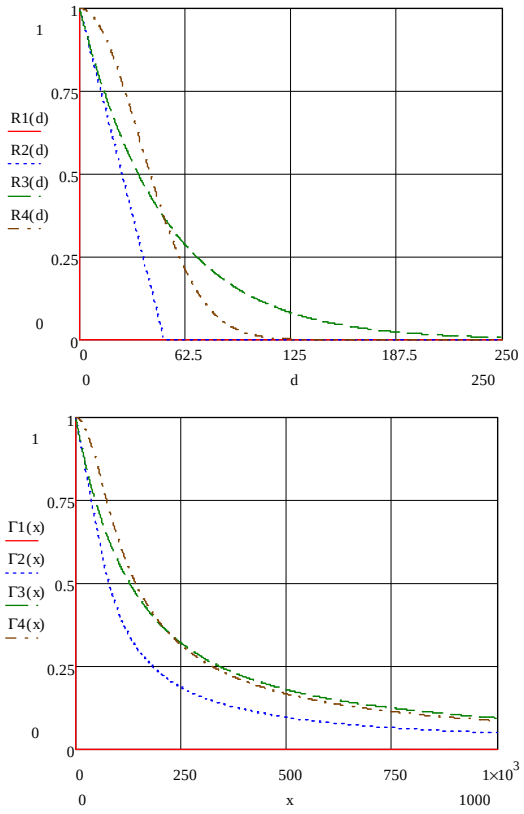

Figure 3 – One-dimensional autocorrelation models and corresponding variance reduction functions

Based on the limited data available, Phoon and Kulhway (1999) concluded that the ratio of the horizontal scale of fluctuation to the vertical one is close to 10, thus confirming the relative greater importance of the latter. The authors suggest that typical values for the horizontal scale vary between 40 m and 60 m. The variability of ϕ and ψ is intimately connected, given the physical relation between both angles.

Table 3 – Variance reduction functions for one-dimensional autocorrelation models

Parameter	Reference	Variation interval	Mean value	COV variation interval (%)	COV mean value (%)
ϕ_{sand}	Lee et al. (1983)	-	-	[5,15]	10
	Phoon & Kulhawy (1999)	[35º,41º]	37.6º	[5,11]	9
ϕ_{clay}	Lee et al. (1983)	-	-	[12,56]	-
	Phoon & Kulhawy (1999)	[9º,33º]	15.3º	[10,50]	21
	Phoon & Kulhawy (1999)	[17º,41º]	33.3º	[4,12]	9
$S_{u,clay}$	Lee et al. (1983)	-	-	[20,50]	30
	Phoon & Kulhawy (1999)*	[15,363] kPa	276 kPa	[11,49]	22
	Phoon & Kulhawy (1999)**	[130,713] kPa	405 kPa	[18,42]	32
$S_{u,sand}$	Lumb (1974)	-	-	[25,30]	30
ρ	Lee et al. (1983)	-	-	[1,10]	3
γ	Phoon & Kulhawy (1999)	[14,20] kN/m^3	17.5 kN/m^3	[3,20]	9
γ_d	Phoon & Kulhawy (1999)	[13,18] kN/m^3	15.7 kN/m^3	[2,13]	7
E	Lee et al. (1983)	-	-	[2,42]	30
p_l^{sand}	Phoon & Kulhawy (1999)	[1617,3566] kPa	2284 kPa	[23,50]	40
p_l^{clay}	Phoon & Kulhawy (1999)	[428,2779] kPa	1084 kPa	[10,32]	15
E_{PMT}	Phoon & Kulhawy (1999)	[5.2,15.6] MPa	8.97 MPa	[28,68]	42

* Unconsolidated undrained test; ** Consolidated undrained test

3.2 Production of simulations via the fast Fourier transform method (FFT)

A local Gaussian variability model with negative exponential spatial correlation was adopted with the purpose of evaluating the relevance of the ground parameters' heterogeneity on the settlements caused by tunnel excavation. Thus, a scalar Gaussian stochastic field $z(x)$ with zero mean, unit variance and scale of fluctuation θ_z was considered. A hundred $z(x)$ realizations were generated, from which the field $E(x)$ was obtained, by translating the mean and scaling the standard deviation:

$$E(x) = \mu_E (1 + z(x) COV_E) \qquad [22]$$

where μ_E and COV_E represent the mean and the coeficient of variation of $E(x)$. The field $\phi(x)$ was obtained from the same realizations $z(x)$.

In order to generate the realizations $z(x)$ four methods could have been used: the turning bands method, the local average subdivision simulation (LAS), the fast Fourier transform method and a technique based on the lower-upper (LU) triangular decomposition of the covariance matrix (Davis, 1987). We opted for the fast Fourier transform method mainly because it is computationally efficient and, being a numerical technique, it can be applied for any given covariance model. Furthermore, the turning bands method could create unwanted anisotropies when a strong anisotropy is present in the geometry of the deposit and the method that considers the LU decomposition of the covariance is only computationally efficient for small grids (up to about 700 points).

The fast Fourier transform method calculates the energy spectrum of the random function from the covariance model and produces a simulation with the appropriate covariance structure in the space domain, by using the fact that the sum of independent multinormally distributed variables is also multinormal.

Any sequence of N values $z(x)$ can be expressed as a finite series of Fourier coefficients, a_j and b_j:

$$z(x) = \sum_{j=0}^{N-1} \left[a_j \cos(2\pi j x / N) + b_j \operatorname{sen}(2\pi j x / N) \right] \qquad [23]$$

for x = 0,…,N-1

Using a complex exponential Fourier series it can equivalently be expressed as:

$$z(x) = F^{-1}(A(j)) = \sum_{j=0}^{N-1} A_j e^{i 2\pi x j / N} \qquad [24]$$

$A_j = a_j - ib_j = |A(j)|e^{-i\varphi(j)}$ is the *j*th complex Fourier coefficient. Its amplitude is $|A(j)| = \sqrt{a_j^2 + b_j^2}$ and its phase is given by $\varphi(j) = \tan^{-1}(-b_j / a_j)$.

The amplitudes $|A(j)|$ are related to the discrete spectral density $s(j)$ or Fourier transform of the Z-covariance by the relation:

$$|A(j)|^2 = s(j) \quad \text{for } j = 0,\ldots,N\text{-}1 \qquad [25]$$

The phase $\varphi(j)$ can be taken as random normally distributed between 0 and 2π, as it doesn't affect the covariance of the series $z(x)$ (Yao, 1998).

The inverse Fourier transform of the complex coefficients $A(j)$ provides the discrete finite realization $z(x)$ ($x = 0,\ldots, N-1$) with the specified covariance spectrum $s(j)$. This inverse discrete Fourier transform can be efficiently computed with the fast Fourier transform.

4. STATISTICAL VARIABILITY OF SETTLEMENTS BASED IN A NUMERICAL MODEL

4.1 Properties of the numerical model

A numerical example was developed to analyze the influence of the ground spatial variability on the deformation around a tunnel opening and on the surface settlements. These variables play a key role in risk management during tunnel construction since alarm and alert behaviour limits are usually expressed in terms of settlement and convergence values. Ground variability effects on settlements have been shown to be more expressive in shallow tunnels (Miranda and Bilé Serra, 2010).

A numerical model of a shallow tunnel excavated in a ground with stationary properties was considered in FLAC 6.0. The ground is 50 m deep overlying a stiff overconsolidated layer. The tunnel diameter is 10 m and the overburden is equal to 15 m. The width of the model is 130 m to prevent the boundary conditions' effect on the tunnel response. Moreover, the distance of the tunnel center to the bottom boundary is three times the diameter.

A Mohr-Coulomb model was selected to simulate the behaviour of the ground (a stiff clay), with a cohesion of 10 KPa. This model takes in consideration the plastification of the ground around the tunnel, which has some influence on the surface settlements. Concerning the deformability modulus, the values considered for μ_E and COV_E were 50 MPa and 20%. In what regards the friction angle, the values assigned to μ_ϕ and COV_ϕ were 28º and 15%.

The realizations $z(x)$ are generated using a MATLAB application. A mesh of 130x50 square elements is defined for the generation of the random field. In what concerns the scale of flutuation, two cases were considered: 4 m and 6 m in the vertical direction and 40 m in the horizontal direction, in accordance to 3.1.3. MATLAB is the leader of the calculation cycle. For each realization of the field z, as described above, a realization of E and ϕ is defined and a system call of FLAC is issued. Statistical analysis of the data, stored in MATLAB arrays, is then performed.

In Figure 4, the values of the deformability modulus as well as the friction angle are represented for realization #53, for θ_z = 4 m and, in Figure 5, for θ_z = 6 m. A greater spatial correlation and consequently less variability of the ground parameters with depth is observed in Figure 5.

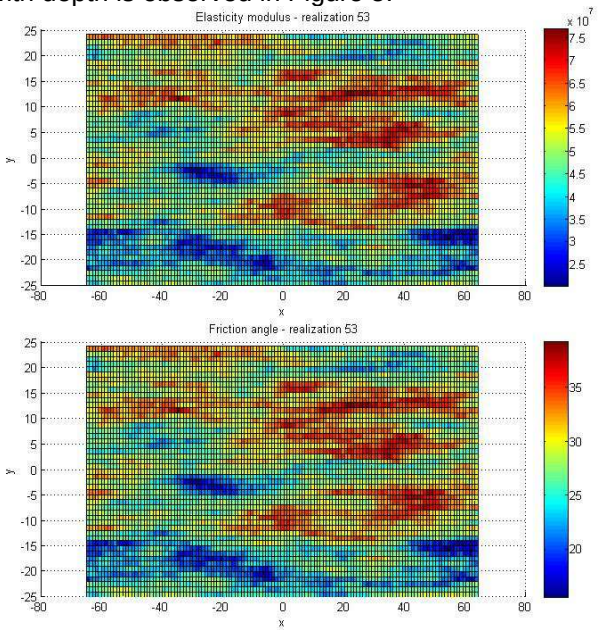

Figure 4 – Deformability modulus and friction angle for realization 53 – θ_z = 4 m

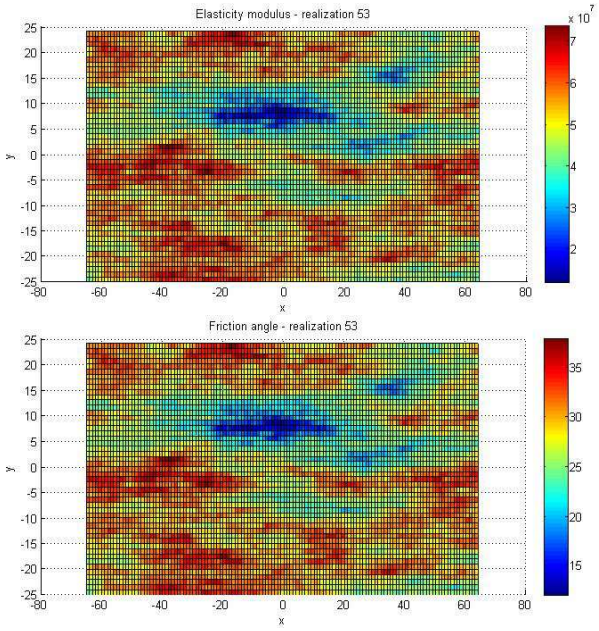

Figure 5 - Deformability modulus and friction angle for realization 53 - θ_z = 6 m

4.2 Analysis of the results

The construction sequence was simulated by the convergence confinement method, with two major

stages: initial equilibrium and full face excavation and partial relaxation at the tunnel periphery, until the support is installed. In order to simulate relaxation, tractions were applied at the tunnel boundary to provide equilibrium at zero relaxation. A relaxation coefficient of 65% was considered to model adequately the behaviour of the ground before support installation.
The output results under analysis are: (i) surface settlements, (ii) a settlement vertical profile from the tunnel crown to the surface and (iii) a convergence profile on the side of the tunnel with an inclination of 45º.

Preceding the one hundred calculations for the random fields, three reference homogeneous models were analyzed, with constant values of E and ϕ': the first with average values, the second with average minus one standard deviation values and the last with average plus one standard deviation values. The above mentioned results are presented in Figure 9, Figure 10 and Figure 11. The peak settlement varies between 7 mm and 21 mm, the crown settlement is between 25 mm and 52 mm, and the 45º half convergence lies between 24 mm and 51 mm. A larger influence of the negative biased parameters (red curves) is observed.

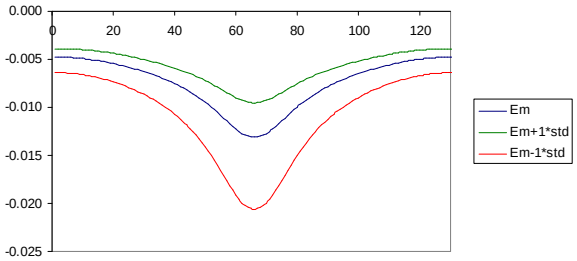

Figure 6 – Surface settlement profile

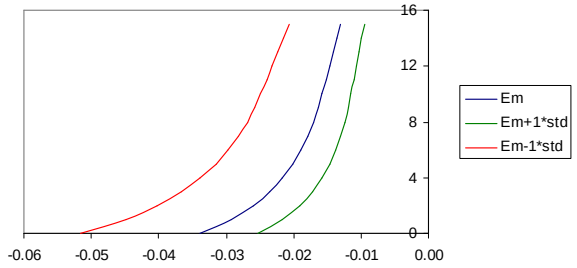

Figure 7 – Vertical displacement profile

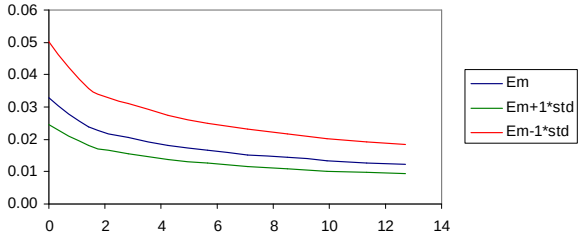

Figure 8 – 45º displacement profile

The results for the one hundred realizations are presented in Figure 9, Figure 10 and Figure 11, respectively, for a vertical scale of fluctuation of 4 m and in Figure 12, Figure 13 and Figure 14, for a vertical scale of fluctuation of 6 m.

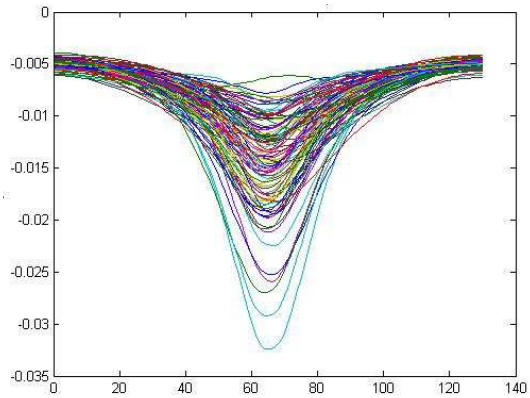

Figure 9 – Surface settlement profile – θ_z = 4 m

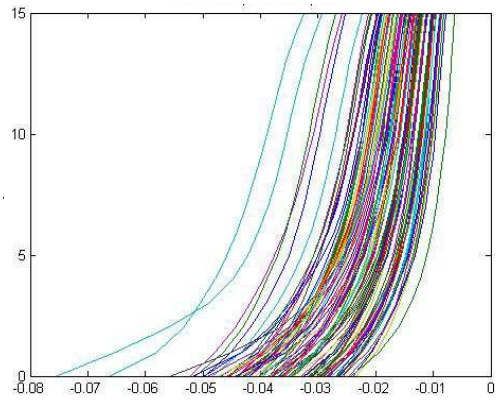

Figure 10 – Vertical displacement profile – θ_z = 4 m

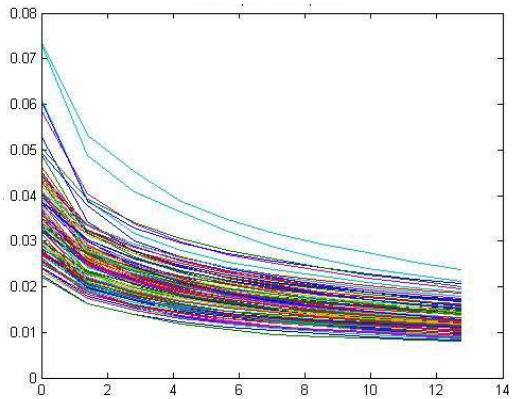

Figure 11 – 45º convergence profile – θ_z = 4 m

The upper 5 % fractile of maximum vertical surface settlement, maximum vertical displacement and maximum 45º displacement corresponds to a value of 2.2 cm, 5.1 cm and 5.3 cm, respectively, for a scale of fluctuation of 4 m. This can be better understood by analyzing the histograms and cumulative frequency curves in Figure 15, Figure 16 and Figure 17.

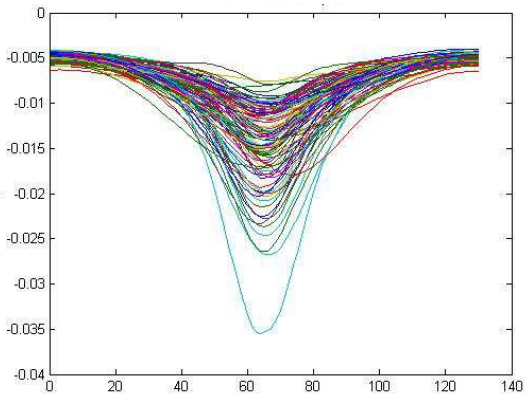

Figure 12 – Surface settlement profile – θ_z = 6 m

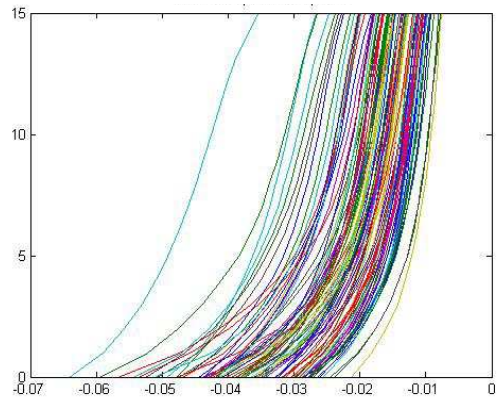

Figure 13 – Vertical displacement profile – θ_z = 6 m

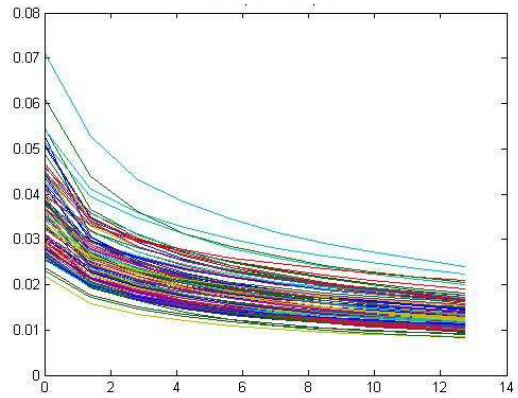

Figure 14 – 45º convergence profile – θ_z = 6 m

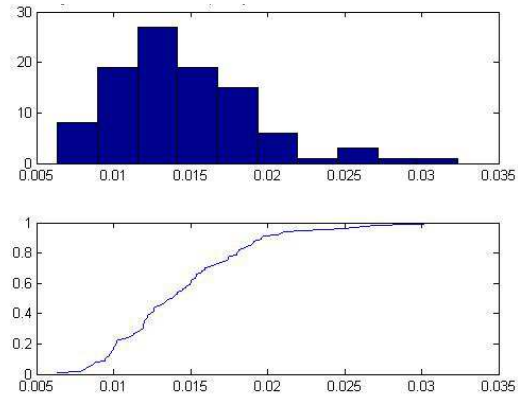

Figure 15 – Histogram and cumulative frequency curve of the maximum surface settlement - θ_z = 4 m

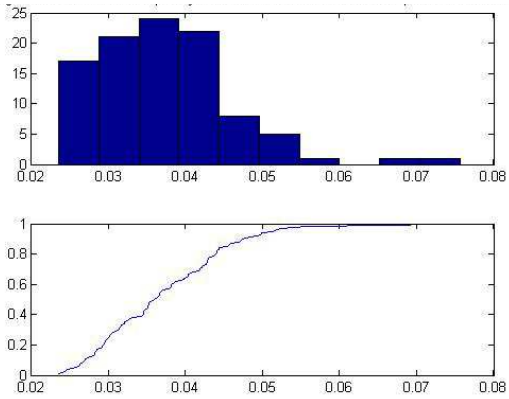

Figure 16 – Histogram and cumulative frequency curve of vertical displacement at the crown - θ_z = 4 m

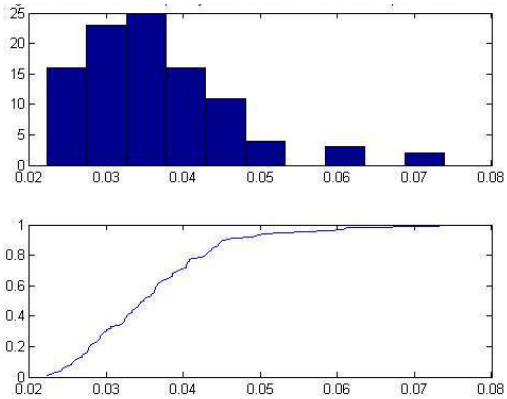

Figure 17 – Histogram and cumulative frequency curve of the maximum 45º convergence - θ_z = 4 m

For the θ_z = 6 m case, the upper 5 % fractile of maximum vertical surface settlement, maximum vertical displacement and maximum 45º displacement corresponds to a value of 2.3 cm, 5.3 cm and 5.1 cm, respectively. The histograms and cumulative frequency curves are shown in Figure 18, Figure 19 and Figure 20.

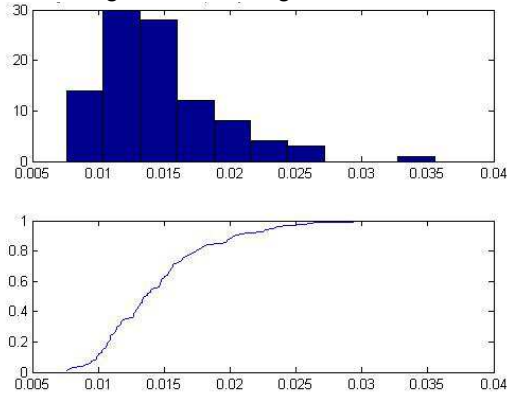

Figure 18 – Histogram and cumulative frequency curve of the maximum surface settlement- θ_z =6 m

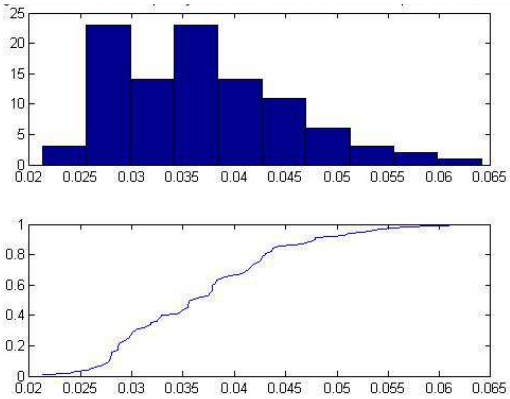

Figure 19 – Histogram and cumulative frequency curve of the vertical displacement at the crown - θ_z = 6 m

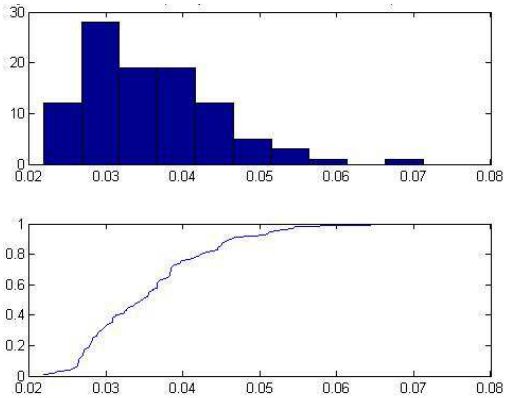

Figure 20 – Histogram and cumulative frequency curve of the maximum 45º convergence - θ_z = 6 m

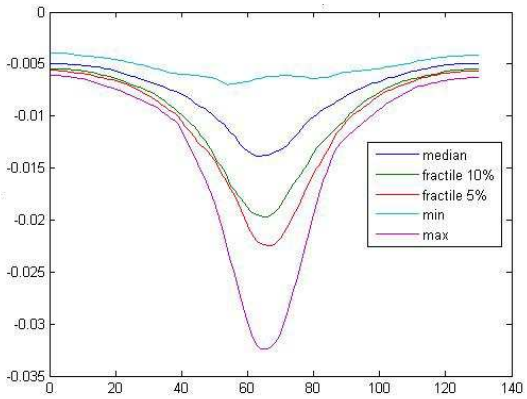

Figure 21 – Statistical curves for the surface settlement – θ_z = 4 m

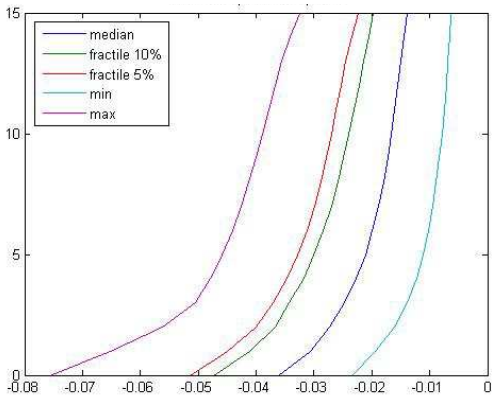

Figure 22 – Statistical curves for the vertical displacement – θ_z = 4 m

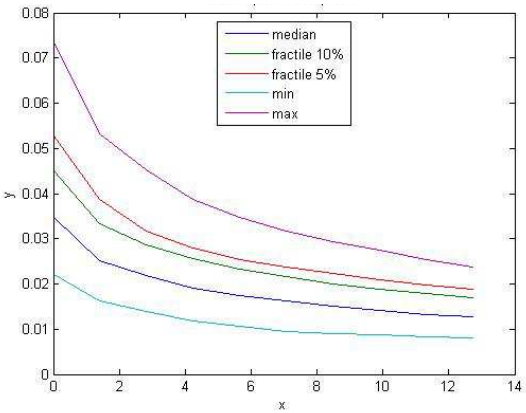

Figure 23 – Statistical curves for the 45º displacement – θ_z = 4 m

A significative scatter was obtained in both cases for the settlement curve at the surface, the settlement profile from the tunnel crown to the surface and the oblique convergence profile. Should the properties' scatter be taken as representative of a current profile with a low density of geotechnical data (due to paucity of in situ tests), it must be considered when defining the alarm and alert limits for the tunnel excavation. As a matter of fact, in the θ_z = 4 m the convergence varies between 44 mm (0.5%D) and 146 mm (1.5%D), the crown setllement varies between 23 mm and 76 mm and the peak surface settlement is between 5 and 32 mm.

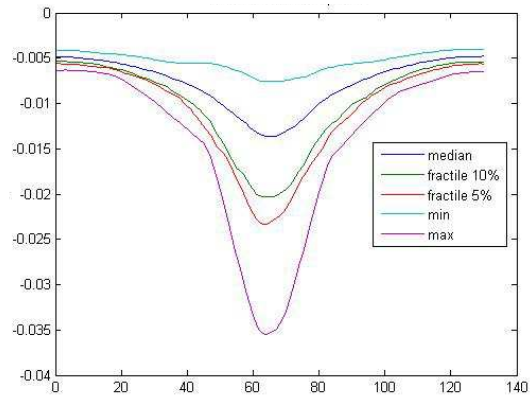

Figure 24 – Statistical curves for the surface settlement – θ_z = 6 m

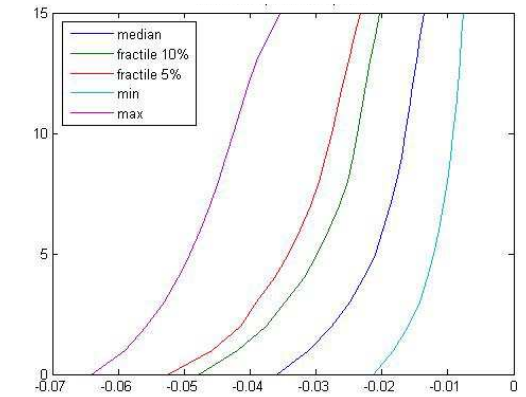

Figure 25 – Statistical curves for the vertical displacement – θ_z = 6 m

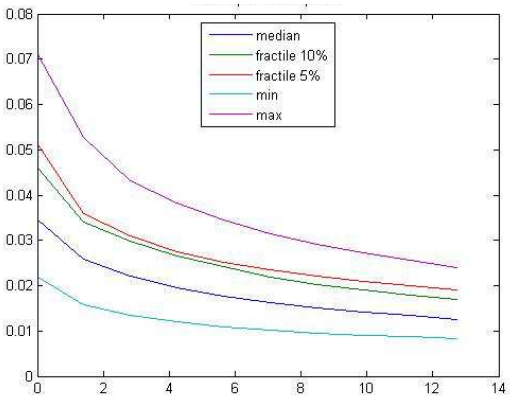

Figure 26 – Statistical curves for the 45º displacement – θ_z = 6 m

5. FINAL CONSIDERATIONS

The present communication addressed the issue of surface settlement caused by tunnelling, given the local and spatial statistical variability of the ground geotechnical parameters.

In what concerns the local variability, it's essential to use analytical expressions for generating realizations of subsidence basins. Thus, the empirical expressions most used to calculate the surface settlements are described and a reference is made to the statistical functions with greater relevance to this problem.

Regarding the spatial variability, the random field theory, associated with the fast Fourier transform method was used to generate realizations of the modulus of deformability and the friction angle of the ground. Two cases were considered for the vertical fluctuation scale – 4 m and 6 m – based in literature values. The influence of both the referred parameters on the ground variability with spatial correlation was then analyzed with regard to the surface settlement, the vertical displacement in a profile linking the top of the tunnel to the surface and the displacements in a profile at 45 degrees with the horizontal axis of the model.

The adopted methodology allows the establishment of characteristic values – upper fractiles – which are useful in defining the criteria for risk management during tunnel construction, when no rupture of the excavation occurs.

6. REFERENCES

Baecher, G. B., Christian, J. T. (2003). Reliability and statistics in geotechnical engineering. John Wiley & Sons, Inc., New Jersey, USA.

Davis, Michael W. (1987). Production of Conditional Simulations via the LU Triangular Decomposition of the Covariance Matrix. Mathematical Geology, Vol. 19, No.2, 91-98.

Franzius (2003). Behaviour of buildings due to tunnel induced subsidence. Ph. D. Thesis, Department of Civil and Environmental Engineering, Imperial College of Science, Technology and Medicine, London.

Lee, K. M., Rowe, R. K., Lo, K. Y. (1992). Subsidence owing to tunnelling. I: Estimating the gap parameter. Can. Geotech. J., Ottawa, Canada, 29, pp. 929-940.

Loganathan, N., Poulos, H. G. (1998). Analytical prediction for tunneling-induced ground movements in clays. Journal of Geotechnical and Geoenvironmental Engineering, Vol. 124, No. 9. pp. 846-856.

Lumb, P. (1974). Application of statistics in soil mechanics. Soil Mechanics: New Horizons. Lee, I. K., ed., London, Newnes-Butterworth, 44–112, 221–239.

Mair, R. J., Taylor, R. N. (1997). Bored tunneling in the urban environment. Proceedings of the 14th International Conference on Soil Mechanics and Foundation Engineering, Hamburg. pp. 2353-2385. Balkema, Rotterdam.

Miranda, L., Serra, J. Bilé (2010). A influência da variabilidade estatística das propriedades do terreno nas estimativas de assentamentos causados pela escavação de túneis. ENESU 2010, Lisboa.

Peck, R. B. (1969). Deep excavations and tunneling in soft ground. Proceedings of the 7th int. Conference on Soil Mechanics and Foundation Engineering. State of the art volume. Pp 225-290. Sociedad Mexican de Mecanica de Suelos, A. C.

Phoon, K-K., Kulhawy, F. H (1999). Characterization of geotechnical variability. Canadian Geotecnhnical Journal, 36, pp. 612-624.

Rowe, R. K., Knack, G. J. (1983). A theoretical examination of the settlements induced by tunnelling: Four case histories. Can. Geotech. J., Ottawa, Canada, 20, pp. 299-314.

Sagaseta, C. (1987). Analysis of undrained soil deformation due to ground loss. Géotechnique 37, No. 3, pp. 301-320.

Schmidt, B. (1969). Settlements and ground movements associated with tunnelling in soil. Ph. D. Thesis, University of Illinois.

Vanmarcke, E. (1984). Random Fields: Analysis and Synthesis. MIT Press, Cambridge. MA.

Verruijt, A., Booker, J. R. (1996). Surface settlements due to deformation of a tunnel in an elastic half plane. Géotechnique 46, No. 4, pp. 753-756.

Yao, Tingting (1998). Conditional Spectral Simulation with Phase Identification. Mathematical Geology, Vol. 30, No. 3, 285-308.